AGU PUBLICATIONS

JGR

Journal of Geophysical Research: Planets

INTRODUCTION TO A SPECIAL SECTION

10.1002/2017JE005401

Special Section:
Investigations of the Bagnold Dune Field, Gale crater

The Mars Science Laboratory (MSL) Bagnold Dunes Campaign, Phase I: Overview and introduction to the special issue

Nathan T. Bridges[1,2] and Bethany L. Ehlmann[3,4]

[1]Applied Physics Laboratory, The Johns Hopkins University, Laurel, Maryland, USA, [2]Deceased 26 April 2017, [3]Division of Geological and Planetary Sciences, California Institute of Technology, Pasadena, California, USA, [4]Jet Propulsion Laboratory, California Institute of Technology, Pasadena, California, USA

Key Points:
- Curiosity's Bagnold Dunes Campaign, Phase I, was the first in situ exploration of an active extraterrestrial dune field
- Wind speed, morphology, grain size, mineralogy, and chemistry were measured over 4 months, interspersed with other rover activities
- Key findings include meter-scale bedforms, saltation at low wind speeds, and particle-size-dependent chemistry, mineralogy, and volatile reservoirs in Martian fines

Correspondence to:
B. L. Ehlmann,
ehlmann@caltech.edu

Citation:
Bridges N. T., and B. L. Ehlmann (2018), The Mars Science Laboratory (MSL) Bagnold Dunes Campaign, Phase I: Overview and introduction to the special issue, *J. Geophys. Res. Planets*, *123*, 3–19, doi:10.1002/2017JE005401.

Received 24 JUL 2017
Accepted 8 SEP 2017
Accepted article online 18 SEP 2017
Published online 9 JAN 2018

Abstract The Bagnold dunes in Gale Crater, Mars, are the first active aeolian dune field explored in situ on another planet. The Curiosity rover visited the Bagnold dune field to understand modern winds, aeolian processes, rates, and structures; to determine dune material composition, provenance, and the extent and type of compositional sorting; and to collect knowledge that informs the interpretation of past aeolian processes that are preserved in the Martian sedimentary rock record. The Curiosity rover conducted a coordinated campaign of activities lasting 4 months, interspersed with other rover activities, and employing all of the rover's science instruments and several engineering capabilities. Described in 13 manuscripts and summarized here, the major findings of the Bagnold Dunes Campaign, Phase I, include the following: the characterization of and explanation for a distinctive, meter-scale size of sinuous aeolian bedform formed in the high kinetic viscosity regime of Mars' thin atmosphere; articulation and evaluation of a grain splash model that successfully explains the occurrence of saltation even at wind speeds below the fluid threshold; determination of the dune sands' basaltic mineralogy and crystal chemistry in comparison with other soils and sedimentary rocks; and characterization of chemically distinctive volatile reservoirs in sand-sized versus dust-sized fractions of Mars soil, including two volatile-bearing types of amorphous phases.

Plain Language Summary Over the course of several months, the Curiosity rover explored the Bagnold dune field in Gale crater, Mars. This was the first time a robotic space mission had visited active, migrating sand dunes on the surface of another planet. In overall dune shape, sand grain size, and dune in migration in the direction of the strongest winds, Curiosity found that dunes on Mars were similar in many ways to those on Earth. But there were also discoveries of key differences that indicate how wind-related processes work. A distinctive type of ripple observed at the Bagnold dunes—sinuous and larger than typical for Earth—may form from conditions specific to Mars' very thin atmosphere. Also, modeling results show that a few grains making short hops cause a large cascade of grain hops -- and thus dune migration -- even at very low wind speeds, a characteristic unique to Mars' low gravity. Unlike what is typical for Earth, the Martian sand grains have different compositions depending on size. Also, the sand dunes are free of the relatively ubiquitous Mars dust, probably due to ongoing wind activity blowing the dust away in suspension. By comparing the chemistries of the dust-free dune sands with more typical sandy-dusty soils, Curiosity discovered elevated sulfur, chlorine, and water in the soils that was easily released by heating. Thus, exploration of the Bagnold dunes revealed many important processes shaping the modern Mars landscape and the chemistry of materials on the Mars surface.

1. Introduction

Planetary science has expanded our understanding of the parameters governing geologic processes and shaping landscape development. Studies once confined to the terrestrial environment are now informed by the broader range of physical conditions, compositions, and geographies obtainable on solid bodies in the solar system, resulting in major progress in virtually all subfields of the geological sciences and related disciplines. Sand dune formation and organization is one such process. Our understanding of the physics of sand transport has grown as models are tested in the lab and in the field on Earth as well as modified to explain the landforms of Mars, Titan, and Venus.

Aeolian sand dunes are accumulations of sand mobilized by the wind. As dynamic landforms, their shape, size, distribution, and migration rate are functions of sediment supply, sediment properties, and wind regime. Active dunes are generally found in arid environments where the relative lack of water (and

vegetation) allows sand mobilization to dominate over processes that promote induration. Terrestrial dunes are dominated by quartz and to a lesser extent feldspar and other minerals, a reflection of the major constituents of Earth's continental crust and their resistance to chemical and physical weathering (in particular, the resistance of quartz). Dunes and their component, superimposed ripples, account for significant portions of the terrestrial sedimentary stratigraphic record, providing clues to ancient environments and sand sources, preserved in rock.

Given that Mars is a world with an atmosphere and a hydrosphere, similar to Earth in terms of geological and environmental processes, water on Mars and its implications for life have received considerable worthwhile attention. Nonetheless, wind stands out among Martian geologic processes as the most active agent of landscape modification today and is analogous in that respect to arid regions on Earth. This is despite Mars' very thin atmosphere, low gravity, cold temperatures, and basaltic-dominated crust—conditions and major compositions that differ markedly from those on Earth. In retrospect, it can therefore be considered both surprising and enlightening that the first Mars orbiter, Mariner 9, discovered vast fields of sand dunes and yardangs [*Marsusky*, 1973], which complemented telescopic observations of local- and global-scale dust storms since the nineteenth century [e.g., *Zurek and Martin*, 1993]. Later higher-resolution images from the Mars Orbiter Camera and the High Resolution Imaging Science Experiment (HiRISE) suggested and then confirmed that many of the dunes were migrating [e.g., *Bourke et al*., 2008; *Silvestro et al*., 2010; *Bridges et al*., 2012; *Ayoub et al*., 2014]. The dunes, although morphologically similar in some respects to those on Earth, also had superimposed ripples of larger size than those found typically found on terrestrial dunes. Surface missions, especially the Mars Exploration Rovers, have investigated, in situ, several types of aeolian features, including ripples, megaripples, dust deposits, and ventifacts [e.g., *Bridges et al*., 1999; *Golombek et al*., 2010; *Greeley et al*., 2002, 2006, 2008; *Jerolmack et al*., 2006; *Sullivan et al*., 2005, 2008].

Complementary to observations of aeolian surface features has been the increasingly detailed Martian stratigraphic record, beginning with geologic maps based on orbital images [e.g., *Scott and Carr*, 1978; *Malin and Edgett*, 2000; *Tanaka et al*., 2014] and advancing to the interpretation of meter-scale stratigraphic sections at subcentimeter spatial scale based on Mars Exploration Rover and later Mars Science Laboratory (MSL) images [e.g., *Edgar et al*., 2012; *Grotzinger et al*., 2005, 2015]. An integral part of these sections are basaltic sandstones, interpreted to have formed in both fluvial, and of relevance here, aeolian regimes. Therefore, as with today, extending billions of years back in Martian history, the transport, deposition, and remobilization of sand by the wind has been a major process.

Prior to arriving at Mars, the mission team recognized that the traverse path of the MSL Curiosity rover would pass through a sand dune field that had previously been shown as active [*Silvestro et al*., 2013]. The region in the vicinity of the rover traverse was informally named the "Bagnold dunes" by the mission team in recognition of the pioneering contributions of British Brigadier Ralph H. Bagnold (1896–1990), who, through his study of bedforms in North Africa and innovative follow-on wind tunnel and theoretical investigations, revolutionized our understanding of aeolian processes on Earth [*Bagnold*, 1941] (Figure 1). It was therefore judged as fitting that we unofficially bestow his name to the first dune field investigated on another planet. Although the overarching strategic approach of MSL was (and is) to ascend Mount Sharp (Aeolis Mons) to assess past environments recorded in the rock strata [*Grotzinger et al*., 2012], the mission team recognized that the opportunity to investigate the Bagnold dune field could be achieved with minimal allocation of time and mission resources. Located parallel to the drive path for 8 km and, indeed, serving as a mobility hazard preventing the direct ascent through Mount Sharp's stratigraphy, the investigation of the dunes waited more than 3 years after MSL's landing in August 2012 until the crossing of the field at a break where sand dunes were not contiguous, thereby permitting ascent up Mount Sharp. During the initial 3 year period, Curiosity's investigation of non-rock targets was limited to soils [e.g., *Cousin et al*., 2015] and inactive bedforms, such as the Rocknest sand shadow [e.g., *Bish et al*., 2013; *Blake et al*., 2013; *Leshin et al*., 2013; *Minitti et al*., 2013] and the Dingo Gap megaripple [*Arvidson et al*., 2017], the properties of which were more representative of evolved Martian soils as opposed to fresh sand. (Here "soils" refer to present-day, loose, fine-grained materials at the Martian surface.) With a sophisticated suite of instruments available for imaging and elemental remote sensing, in situ chemistry and mineralogy, microscopic imaging, and environmental monitoring (Table 1), Curiosity was better suited than any previous Mars mission to mount a series of investigations to address fundamental questions about Martian sand dunes, centered on their current state, dynamic evolution, and ties to the planet's geologic history.

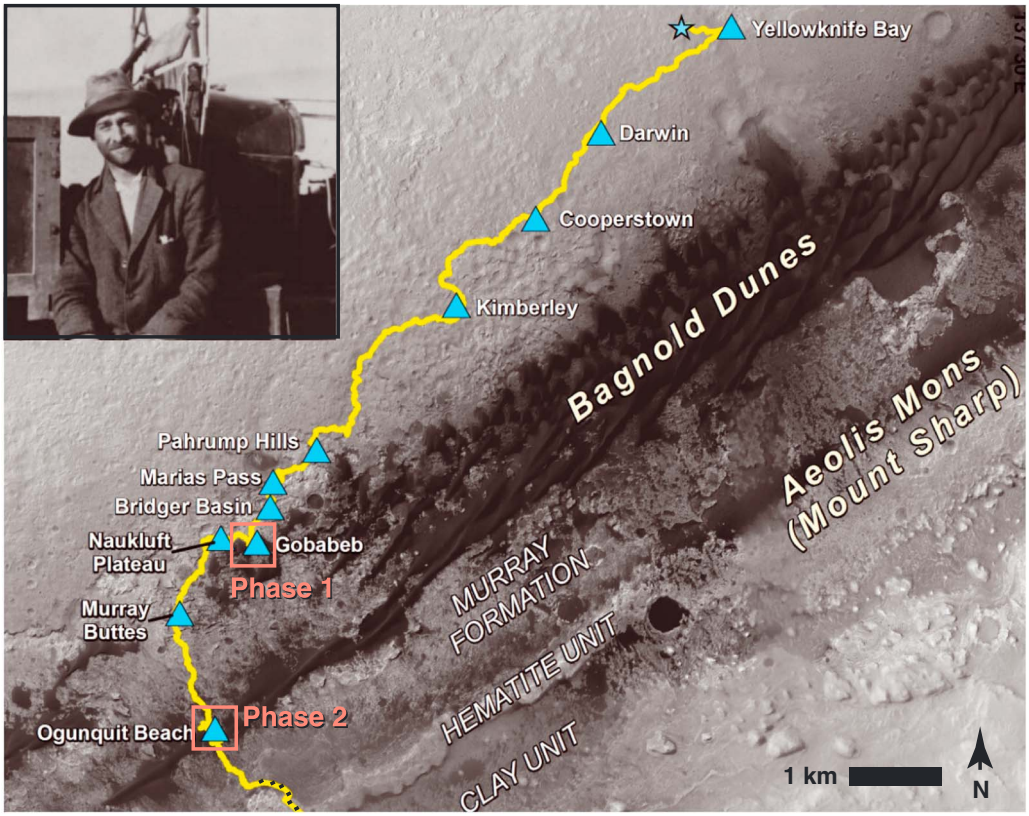

Figure 1. The Curiosity rover traverse with key locales and the locations of Phase 1 and Phase 2 of the Bagnold Dune Campaign highlighted. (inset) Ralph A. Bagnold (photo reprinted from his memoir [*Bagnold*, 1990], courtesy of Stephen Bagnold).

Table 1. MSL Instruments and Systems Which Carried out the Investigations at the Bagnold Dunes

Abbreviation	Instrument (Type)	Instrument Reference
APXS	Alpha-Particle X-ray Spectrometer (X-ray instrument for elemental chemistry)	*Gellert & Clark* [2015]
CheMin	Chemistry and Mineralogy (XRD, X-ray diffraction instrument for mineralogy)	*Blake et al.* [2012]
ChemCam	Chemical Camera (LIBS, laser-induced breakdown spectrometer, and RMI, remote microscopic imager, for elemental chemistry and imaging)	*Maurice et al.* [2012], *Wiens et al.* [2012]
DAN	Dynamic Albedo of Neutrons (pulsing neutron generator and neutron detector for measurement of subsurface hydrogen content)	*Mitrofanov et al.* [2012], *Sanin et al.* [2015]
Engineering cameras (Navcam and Hazcam)	Navigation Cameras (mast-mounted stereo cameras for imaging) and Hazard Avoidance Cameras (wide field-of-view stereo cameras beneath the rover for imaging)	*Maki et al.* [2012]
MAHLI	Mars Hand Lens Imager (focusable macrolens color camera on the rover arm for close-up imaging)	*Edgett et al.* [2012]
MARDI	Mars Descent Imager (downward-facing color camera for imaging)	*Malin et al.* [2017], *Bell et al.* [2017]
Mastcam	Mast Cameras (focusable, mast-mounted stereo color cameras with 12 visible/near-infrared filters for imaging and color/spectral analysis)	*Malin et al.* [2017], *Bell et al.* [2017]
REMS	Rover Environmental Monitoring Station (air and ground temperature, pressure, relative humidity, wind speed, and ultraviolet radiation sensors)	*Gomez-Elvira et al.* [2012]
SAM	Sample Analysis at Mars (gas chromatograph, mass spectrometer, and tunable laser spectrometer for volatile content and isotopic composition)	*Mahaffy et al.* [2012]
SASPaH	Sample Acquisition, Sample Processing and Handling System (for preparation of samples for analysis by other rover instruments)	*Anderson et al.* [2012]

2. Investigation of the Bagnold Dune Field With the Curiosity Rover: Motivating Science Questions and Objectives

Reflecting the unique opportunity afforded by the first extraterrestrial dune study and to properly plan Curiosity's activities, the mission team organized science questions within broad, overlapping science goals: (1) understand current dune processes, rates, and structures; (2) constrain dune material chemical and physical properties and determine the extent and type of compositional sorting of dune materials; and (3) use knowledge gained to decipher past aeolian processes preserved in Mars' rock record, relating the modern dunes to the paleosedimentary rock record, including similarities in sediment sources and sinks and any geochemical alteration.

Several key questions were motivated by existing knowledge, obtained with remote sensing. Orbital data had shown that the Bagnold dunes exhibited variable morphology with barchan dunes at the margins feeding into longitudinal dunes in the core of the field. The dunes were active, migrating at rates of 0.4 m/Earth-year [*Silvestro et al*., 2013]. Furthermore, the dunes exhibited ripples of multiple size scales. This motivated questions of dynamics and structure such as (i) what are the rates and fluxes of active Martian dunes in both the bulk dune and constituent ripples, and what wind speeds generate this flux? and (ii) what is the morphology/structure and formation mechanism(s) of dune ripples and the causes of differences from terrestrial dunes? Based on orbital data, it had also long been recognized that the dunes were distinctly olivine-bearing and basaltic in composition [*Pelkey et al*., 2004; *Rogers and Bandfield*, 2009; *Anderson and Bell*, 2010; *Milliken et al*., 2010; *Lane and Christensen*, 2013]. More recently, high spatial and spectral resolution CRISM (Compact Reconnaissance Imaging Spectrometer for Mars) data had shown variations in the spectral properties of dunes within the field (comparatively olivine-enriched margins relative to the more pyroxene-enriched core) and relative to the surroundings (the dunes are relatively dust-free) [*Seelos et al*., 2014]. With regard to composition, key questions included (i) to what extent are winds mineralogically sorting the sands? and (ii) how does Martian sand mineralogy and volatile content vary with grain size? Lastly, orbital (and later in situ) data showed aeolian sandstone units in Mount Sharp and on the Gale crater floor [*Anderson and Bell*, 2010; *Milliken et al*., 2010; 2014; *Le Deit et al*., 2013; *Buz et al*., 2017]. Investigation of modern Martian sand dunes offered an opportunity to examine the structures and chemistry of aeolian sediments prior to lithification and diagenesis. In addition to the science questions above, the Bagnold dunes presented an opportunity to ground truth these remote sensing data, examining how inferences from orbit were confirmed (or not) in the select areas of the dune field examined on the ground.

The broad goals and key questions were then translated into measurement objectives achievable with the rover payload. Addressing these measurement objectives required coordinated rover observations and measurements using the rover science instruments, which are listed in Table 1 with instrument abbreviations defined:

1. *Determine the size, shape, and characteristics of dune structures (Mast Cameras (Mastcam) and Navigation Cameras (Navcam))*. Sedimentary structures of the dunes and superimposed ripples were imaged with Navcam and Mastcam in stereo and at a variety of angles. Navcam was mostly used to provide context and refine the pointing of subsequent Mastcam images. Stereo image data were also used to derive digital elevation models to compute surface topography and volumes. The rover wheel was used to scuff into dune sands, effectively sectioning ripples to look for phenomena like armoring or layering.
2. *Measure the size and shape of Martian dune sands as a function of location (Chemical Camera-remote microscopic imager (ChemCam-RMI), Mars Hand Lens Imager (MAHLI), and Mastcam)*. The size and shape of sand grains were determined from close-up images. In the case of Mastcam and RMI, which are located on the rover mast, typical close-in imaging distances were ~2.5–3 m, resulting in pixel scales of ~185–225 μm and ~50–60 μm, respectively. To get finer details required close-up images with MAHLI, located on the rover arm. At the closest 0.5 cm standoff distances, pixel scales of ~14 μm were achieved.
3. *Determine the rates of changes at the dunes and associated threshold wind speeds (ChemCam-RMI, Mastcam, and Rover Environmental Monitoring Station (REMS))*. Changes were determined by imaging the same location over several Martian solar days (sols) or, in some cases, staggered times within a single sol. Mastcam was the most common camera used, and RMI was used occasionally to provide the highest resolution at long distances. For intrasol change detection, extended sessions of REMS were scheduled to bridge some of the images so that any grain movement and other activity could be tied to 1 Hz wind measurements.

4. *Determine the chemical composition, mineralogy, and volatile content of dune sands, including variation with grain size (Alpha-Particle X-ray Spectrometer (APXS), ChemCam-laser-induced breakdown spectrometer (LIBS), CheMin, Dynamic Albedo of Neutrons (DAN), and Sample Analysis at Mars (SAM))*. This suite of compositional measurements required positioning the rover so that sands were accessible by multiple instruments but not so close that deep sands presented a threat to rover mobility. Sands needed to be ~2–3 m away from the front of the rover to make the sands reachable with the rover arm for APXS elemental chemistry and for scooping by the sample handling system for delivery to SAM and CheMin but far enough away ($>$ ~2 m) to perform ChemCam elemental chemistry measurements with the LIBS laser in focus. The sands had to be more than a few centimeters deep to enable ample sand for safe scooping. The Bagnold dune sands were the first opportunity to utilize the rover's sampling system to sieve materials into different grain size fractions and then measure their compositional properties as a function of size. APXS measured the elemental composition of piles of sand with different grain size distribution, hovering over piles on the Martian surface that were generated by the sample handling system. The SAM instrument was used to study the temperatures of release of volatiles, their quantities, and their isotopic composition, comparing the results from fine ($<$150 μm) versus coarse ($<$150 μm–1 mm) sieved sands. The CheMin mineralogy data and SAM data volatile chemistry data were compared with Martian soils measured previously at the inactive bedform Rocknest. As the last compositional measurement, the rover was reoriented backward so as to place the DAN measurement footprint over the dune sands in order to measure the hydrogen content of the sands.
5. *Measure the remote sensing signature of the dune sands (ChemCam-passive, Mastcam, and REMS)*. Dune sands were measured in the ultraviolet to visible/near-infrared (VNIR) spectral range using the ChemCam spectrometers in passive mode and by acquisition of VNIR multispectral images with Mastcam. The REMS ground temperature sensor measured infrared radiance at multiple times of day from which temperature and substrate thermophysical properties can be derived.

3. Implementation: Rover Traverse and Activities

The Bagnold Dune Campaign was divided into two main phases, for which Phase I is the focus of this special issue. It spans sols 1162 to 1254, taking place from 11 November 2015 to 14 February 2016. (A sol for the Curiosity rover is defined as the number of Mars days since landing on 5 August 2012). Phase II, within longitudinal dunes to the south, was recently completed as of this writing and will be the subject of future papers.

An active barchanoidal dune, Namib (Figure 2), whose motion was observed from orbital instruments, was chosen as the principal stop for investigations of the active part of the dune field. The original Phase I campaign plan had a second stop for sampling and detailed compositional studies at a relatively inactive part of the dune field, Kalahari Dune, which was dusty and not observed from orbit to be migrating. The intent was to characterize changes in composition and grain size as a function of activity. But the Kalahari Dune stop was removed when the strategic traverse path of the rover changed, placing the relatively inactive dunes far enough away that a detour for measurement would require a couple weeks of dedicated driving. Consequently, measurements of inactive sands in the dune field were not undertaken, in favor of the expeditious route through Mount Sharp stratigraphy.

The Bagnold Dune Campaign Phase I, as implemented, was partitioned into seven subphases defined by location, engineering operations, and major science activities (Figure 2). Important events on each sol within these blocks are tabulated (Table 2). The subphases of the campaign are briefly described here, with details of some of the major science operations more fully explained in several of the contributions to this special issue.

3.1. Subphase 1: Entering the Dunefield (Sols 1162–1181)

Curiosity's path through the dune field started with an approach from the north, with three stops, on sols 1162, 1167, and 1168 in which the rover parked in roughly equally separated azimuths (314.2°, 193.1°, and 75.7°, respectively) to allow REMS to comprehensively assess the local horizontal wind field apart from the influence of the dunes. Mastcam imaging and ChemCam passive VNIR spectroscopy of High and Namib Dunes were performed. SAM and CheMin were prepared to receive the sand samples by acquisition of data needed for later calibrations. Other activities related to analyses of rocks were also performed during the traverse to the dune field.

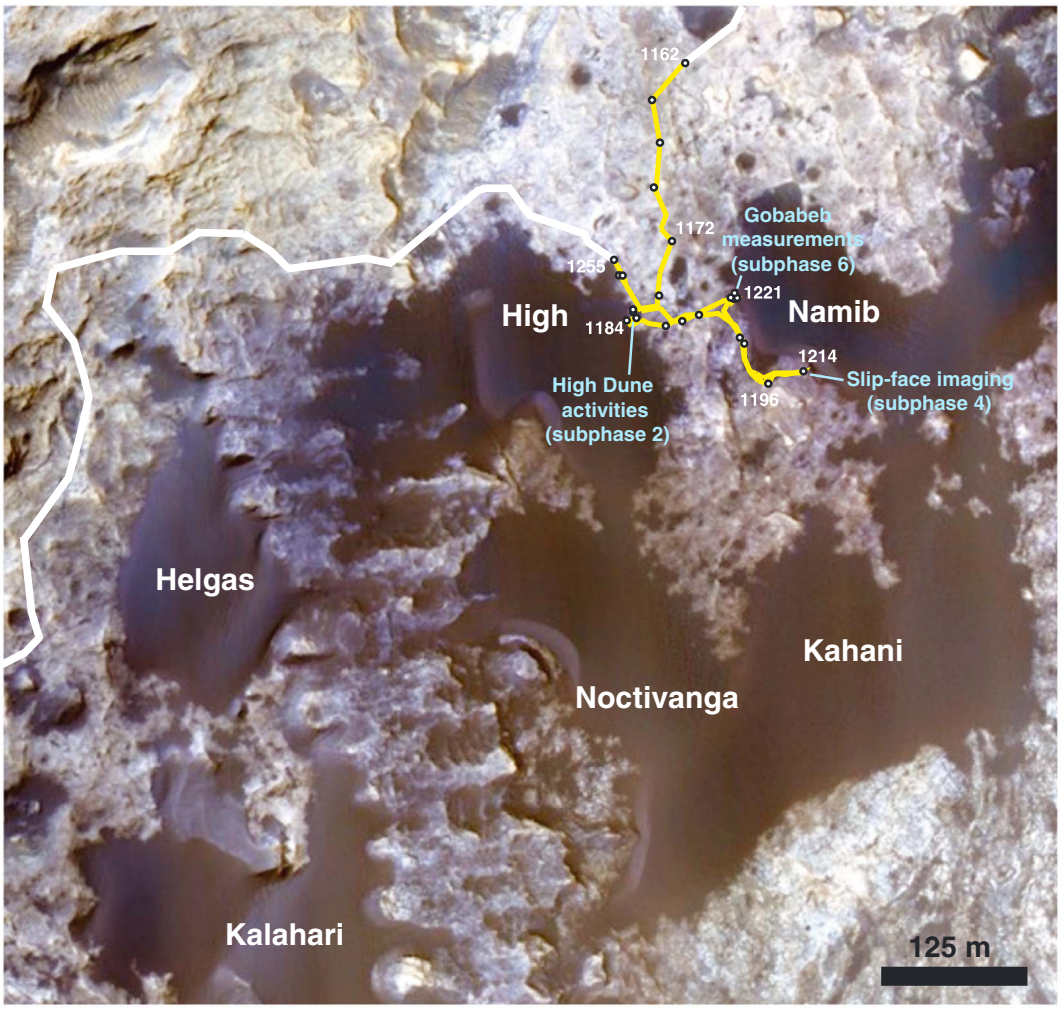

Figure 2. HiRISE color image mosaic with the rover traverse (white), colored yellow over the period where activities associated with the Bagnold Dune Campaign, Phase 1, took place. Dune and target names for Mars are taken from the Namib desert and surrounding areas on Earth.

3.2. Subphase 2: Engineering and Science Activities Near and at High Dune (Sols 1181–1185)

Sand patches near High Dune were judged by the rover engineering team as convenient, accessible locations for tests of the rover's ability to drive within sands. At a distance of 8 m east of High Dune, Curiosity did a test of mobility on basaltic sand by driving over a ripple, after which MAHLI and APXS measurements were made of undisturbed (Warsaw, near ripple crest) and wheel-disturbed (Weissrand) areas. Two ChemCam targets were also measured in the disturbed area (Awasib and Hoanib). The rover then drove next to High Dune, conducted a second mobility test on the dune sand, and did MAHLI, APXS, and ChemCam near the crest of a large ripple (Barby) and trough between two smaller ripples (Kibnas).

3.3. Subphase 3: Drive From High Dune to Namib Dune (Sols 1185–1196)

Curiosity left High Dune and drove toward the slip face of Namib Dune. Activities included targeted remote sensing of the dunes and investigation of interdune bedrock targets.

3.4. Subphase 4: Namib Dune Slip Face and December–January Holidays (Sols 1196–1215)

While readying for the break in regular operations during the December–January holiday season of 2015–2016, measurements were made of the Greenhorn rock sample, acquired earlier in the mission (not part of the Bagnold dune campaign). Additionally, remote sensing of the dunes and preparatory activities to ready the rover for the break in tactical operations were performed. For 9 sols over the holiday break when regular daily uplink and downlink operations were on leave, the rover was parked 15 m from the slip face of Namib

Table 2. A Summary of Bagnold Campaign Activities by Sol with Science-Related Activities in Normal Typeface and Engineering-related Activities in Italics

Sol	Summary of Activities While in the Vicinity of the Bagnold Dunes	Instruments Used for Bagnold Campaign Measurements[a]
Subphase 1: Entering the Dunefield (Sols 1162–1181)		
1162	Drive toward Bagnold Dunes; REMS dune campaign observations; Remote sensing	ChemCam LIBS, passive
1163	REMS dune campaign observations; remote sensing	Mastcam
1164	*Science runout (Deep Space Network issue; plan uplink was not successful)*	
1165	*Science runout (Deep Space Network issue; plan uplink was not successful)*	
1166	Brush Swartkloofberg rock target with dust removal tool and in situ observations; targeted remote sensing; SAM instrument getter scrubber cleanup	
1167	Drive toward Bagnold Dunes, REMS dune campaign observations; targeted remote sensing, including Mastcam color and ChemCam passive of dunes	Mastcam, ChemCam LIBS, passive
1168	Drive toward Bagnold Dunes, REMS wind calibration; targeted remote sensing; SAM atmospheric methane measurement	Mastcam
1169	Targeted remote sensing, including Mastcam color of Namib Dune and High Dune	Mastcam, ChemCam, LIBS
1170	Remote Sensing; SAM instrument preconditioning	
1171	Targeted remote sensing, including Mastcam and Navcam of the dunes; CheMin cleaning activities; SAM evolved gas analysis blank	Mastcam
1172	Drive toward Bagnold Dunes; remote sensing	
1173	Drive toward Bagnold Dunes, targeted remote sensing, including of dunes; *RCE-A maintenance activity*	Mastcam
1174	Drive toward Bagnold Dunes; CheMin sample dump and empty cell analysis; targeted remote sensing, including of dunes	Mastcam, ChemCam LIBS, passive
1175	CheMin empty cell analysis; remote sensing	
1176	CheMin empty cell analysis; remote sensing	Mastcam
1177	Targeted remote sensing, including of dune sands; SAM preconditioning	Mastcam, ChemCam LIBS, passive
1178	Remote sensing; SAM sample drop-off of cached sample and analysis	Mastcam
1179	Full MAHLI wheel imaging; remote sensing	
1180	*Science Runout (DSN issue; plan uplink was not successful)*	
Subphase 2: Engineering and Science Activities Near and at High Dune (Sols 1181–1185)		
1181	Bump to test location; rover sand mobility testing; *engineering activities*; remote sensing, including of dunes	Mastcam
1182	*Rover sand mobility testing*; MAHLI and APXS of undisturbed sand (Warsaw), wheel tracks (Weissrand), MAHLI tracks imaging, MAHLI wheel imaging; targeted remote sensing	Mastcam multispectral, ChemCam LIBS, passive, MAHLI, APXS
1183	*Rover sand mobility testing*; drive to High Dune; targeted remote sensing	Mastcam multispectral
1184	MAHLI and APXS of ripple trough (Kibnas) and Ripple Crest (Barby) targets, MAHLI observations of CheMin inlet; targeted remote sensing	Mastcam, ChemCam LIBS, passive, MAHLI, APXS
Subphase 3: Drive From High Dune to Namib Dune (Sols 1185–1196)		
1185	Drive toward Namib Dune; targeted remote sensing	
1186	Remote sensing	
1187	Drive toward Namib Dune; targeted remote sensing; *RCE maintenance*	
1188	Untargeted remote sensing; SAM electrical baseline test	
1189	Targeted remote sensing	
1190	Targeted remote sensing, including of dunes; *thermal characterization of non-prime power and analog module*	Mastcam
1191	In situ observations of Pomona and Elizabeth Bay rock targets; targeted remote sensing; *Battleshort checkout*	
1192	Drive toward lee side slip-face of Namib dune; targeted remote sensing, including of dunes; *Battleshort checkout*	Mastcam
1193	Remote sensing	
1194	Drive toward lee side slip-face of Namib dune; targeted remote sensing, including of dunes	Mastcam
1195	REMS maintenance activity; remote sensing	
Subphase 4: Namib Dune Slip Face and December–January Holidays (Sols 1198–1215)		
1196	Drive toward lee side slip-face of Namib dune; targeted remote sensing, including of the dunes	Mastcam, ChemCam
1197	Remote sensing	Mastcam
1198	MAHLI imaging of rock surface; targeted remote sensing, including of the dunes	Mastcam, ChemCam RMI
1199	Targeted remote sensing, including of the dunes	ChemCam RMI
1200	Targeted remote sensing, including of the dunes	Mastcam, ChemCam RMI
1201	Targeted remote sensing, including of the dunes; rover arm diagnostics	Mastcam, ChemCam RMI
1202	Greenhorn drill powder sample dump; in situ observations of dump pile; *Battery thermal characterization*; targeted remote sensing, including of the	Mastcam, ChemCam RMI
1203	MAHLI observations of Greenhorn drill fines pile, *battery thermal characterization*; targeted remote sensing, including of the dunes	Mastcam, ChemCam

Table 2. (continued)

Sol	Summary of Activities While in the Vicinity of the Bagnold Dunes	Instruments Used for Bagnold Campaign Measurements[a]
1204	Bump for REMS activities; targeted remote sensing; SAM calibration activities	Mastcam
1205	REMS Science (*Earth Christmas-New Year's holiday*)	
1206	Remote sensing, including of dunes (*Earth Christmas-New Year's holiday*)	Mastcam, Navcam
1207	REMS science (*Earth Christmas-New Year's holiday*)	Mastcam
1208	REMS science (*Earth Christmas-New Year's holiday*)	
1209	REMS science (*Earth Christmas-New Year's holiday*)	
1210	Remote sensing, including of dunes (*Earth Christmas-New Year's holiday*)	Mastcam, Navcam
1211	REMS science (*Earth Christmas-New Year's holiday*)	Mastcam
1212	REMS science (*Earth Christmas-New Year's holiday*)	
1213	REMS science (*Earth Christmas-New Year's holiday*)	
1214	MAHLI wheel imaging; targeted remote sensing, including of dunes	Mastcam
Subphase 5: Traverse to Namib Dune: Slip Face to Gobabeb (Sols 1215–1221)		
1215	Drive toward Gobabeb secondary slip face; remote sensing, including of dunes	
1216	Drive toward Gobabeb secondary slip face; remote sensing	Mastcam
1217	*Rover Motor Controller Assembly Anomalies Preclude Science Observations*	
1218	*Science Runout (RMCA anomaly precluded execution of intended plan)*	
1219	Targeted remote sensing, including of dunes; *RMC-A diagnostic activities*	Mastcam
1220	Targeted remote sensing, including of dunes; *RMC-A diagnostic activities*	Mastcam
Subphase 6: Intensive Coordinated Measurement Campaign at Gobabeb (Sols 1221–1244)		
1221	Arrive Gobabeb; Bump to and scuff Gobabeb target, *Battleshort checkout*; targeted remote sensing; SAM atmospheric measurement	Mastcam
1222	Targeted remote sensing	Mastcam
1223	MAHLI and APXS of Gobabeb scuff; MAHLI of scoop locations; remote sensing; SAM preconditioning	Mastcam, MAHLI, APXS
1224	Scoop and sieve Gobabeb sand (<150 μm); remote sensing; SAM sample drop-off and analysis	Mastcam, SAM <150um fraction
1225	In situ observations of undisturbed sand near the Gobabeb scoop with APXS; targeted remote sensing	Mastcam, Chemcam LIBS, APXS
1226	CheMin sample drop-off of <150 μm sands; dump sieved materials to produce piles A and B; MAHLI observations of Gobabeb scoop, scuff, and discard pile B; APXS pile A; targeted remote sensing	Mastcam, MAHLI, APXS
1227	CheMin analysis of Gobabeb scoop sample; MAHLI observations of Gobabeb discard pile A; targeted remote sensing	Mastcam, MAHLI, CheMin
1228	MAHLI selfie; scoop and sieve Gobabeb sands to 150 μm–1 mm fraction; creation of discard piles C and D; MAHLI observations of scoops, scuff, and discard piles A and B; targeted remote sensing	Mastcam, MAHLI
1229	Targeted remote sensing, including ChemCam of discard piles A, B, C, D; *thermal characterization of non-prime power and analog module*	Mastcam, ChemCam LIBS, passive
1230	MAHLI of discard piles A, B, C, D; APXS of discard pile D; targeted remote sensing; SAM preconditioning and sample drop-off of the coarse fraction	MAHLI, APXS
1231	Scoop and sieve Gobabeb target (*arm actuator fault precludes processing and delivery of second portion of coarse fraction to SAM; APXS dump C precluded*)	
1232	*Anomaly state precludes most activities*	
1233	*Anomaly state precludes arm activity execution*; remote sensing,	Mastcam, ChemCam LIBS
1234	*Anomaly state precludes arm activity execution*; remote sensing,	Mastcam, Chemcam LIBS, passive
1235	Arm diagnostics; targeted remote sensing, including of dunes	Mastcam, Navcam, Chemcam LIBS, RMI
1236	Targeted remote sensing, including of dunes	Mastcam, Navcam, ChemCam LIBS (overnight)
1237	*CHIMRA diagnostics; targeted remote sensing, including of dunes*; SAM analysis of Scoop 2 sample (single portion, coarse fraction)	Mastcam, SAM 150um-1mm fraction (single portion only)
1238	Targeted remote sensing, including of dunes	Mastcam
1239	CheMin analysis of Gobabeb scoop sample; arm diagnostics; targeted remote sensing; CheMin Gobabeb	Mastcam, ChemCam LIBS, CheMin
1240	Targeted remote sensing, including of dunes; SAM electrical baseline test	Mastcam
1241	APXS discard pile C; MAHLI close observation discard pile A; MAHLI Otavi target, piles C and D, Gobabeb workspace; targeted remote sensing, including of dunes; *CHIMRA diagnostics*	Mastcam, MAHLI, APXS
1242	APXS discard piles B and C (redo); MAHLI close observations of Gobabeb discard piles B, C, D, and Otavi target; targeted remote sensing; *CHIMRA diagnostics*	Mastcam, ChemCam RMI, MAHLI, APXS
1243	Drive to position for DAN Active; DAN active of dunes; CheMin analysis of Gobabeb scoop sample; postdrive remote sensing; *CHIMRA diagnostics*	DAN completely over dune, CheMin
1244	Depart Gobabeb site; drive away imaging wheel tracks in sand; arrive at bedrock contact science location; targeted remote sensing, including	Mastcam
…	interlude in Bagnold Campaign-related activities; assorted drive and science activities	

Table 2. (continued)

Sol	Summary of Activities While in the Vicinity of the Bagnold Dunes	Instruments Used for Bagnold Campaign Measurements[a]
Subphase 7: Measurement of Final Gobabeb Discarded Sand Piles (Sols 1251–1254)		
1251	Discard remaining Gobabeb sample, MAHLI observations of discard piles E and F; Brush and in situ observations of Kuiseb rock target; targeted remote sensing; SAM atmospheric activities	MAHLI
1252	APXS of its calibration target; targeted remote sensing	
1253	MAHLI and APXS observations of sand discard piles E and F, Kuiseb and Bergsig rock targets; targeted remote sensing; *CHIMRA diagnostics*	MAHLI, APXS, ChemCam passive
1254	CheMin analysis of Gobabeb scoop sample; MAHLI observations of Kuiseb target, discard pile E; APXS vibration cleaning; targeted remote sensing	Mastcam, ChemCam LIBS, MAHLI, CheMin

[a]Note that engineering camera images (Navcam, Hazcam) were frequently acquired and REMS environmental monitoring was performed throughout.

Dune, affording the opportunity to undertake long-term change detection observations. REMS provided measurements showing the influence of the dune on wind recirculation.

3.5. Subphase 5: Traverse to Namib Dune: Slip Face to Gobabeb (Sols 1215–1221)

Curiosity next drove northwest toward Gobabeb, a site at the western secondary slip face of Namib Dune. Targeted remote sensing was undertaken, including change detection of the sand target Solitaire.

3.6. Subphase 6: Intensive Coordinated Measurement Campaign at Gobabeb (Sols 1221–1244)

After the holidays, the rover drove toward Gobabeb, the prime site for in situ measurement as well as dealt with unexpected vehicle anomalies. The secondary slip face of Namib dune was chosen because of a combination of access to enable all measurements (see section 2) and characteristic dune properties seen from orbit (for further detail on this site, activities, and production of samples see section 2.1 in *Ehlmann et al.* [2017]). The first activity was to use the rover wheels to scuff into the dune, revealing interior ripple stratification and allowing both interior and surface compositions of sand to be measured. Over subsequent sols, MAHLI and APXS measurements were taken of the scuff and of undisturbed sands, which were given the target name Otavi. Sands were also scooped and sieved to deliver a $<$150 μm fraction to CheMin and $<$150 μm and 150 μm–1 mm fractions to SAM, the first time the latter fraction was sampled on Mars. An arm fault occurred during the activity to produce the 150 μm–1 mm sand, so only a smaller-than-expected portion was ingested in SAM. The rover sampling system was also used to produce discard piles of $<$150 μm sand, $>$150 μm sand, and 150 μm–1 mm sand (respectively, Piles A, B, and C; an intended Pile D with $>$1 mm sands did not produce this fraction due to the lack of large grains). These piles were measured with APXS and MAHLI. Additional activities included MAHLI UV illumination measurements to look for mineral or organic fluorescence, remote sensing with Mastcam and ChemCam, change detection imaging observations of the slump deposit Hebron with Mastcam and ChemCam RMI, and use of DAN in its active and passive modes to assess hydrogen content of the dune sands.

3.7. Subphase 7: Measurement of Final Gobabeb Discarded Sand Piles (Sols 1251–1254)

After traversing to bedrock on the northeast edge of High Dune and at a time when analyses were convenient to other activities unaffiliated with the dunes campaign, the $<$150 μm (Pile E) and $>$150 μm (Pile F) portions of Scoop 3 (from when processing failed for SAM delivery) were discarded on the surface. MAHLI, APXS, Mastcam, and ChemCam passive observations of these piles on sols 1253–1254 and continued CheMin analysis of the $<$150 μm material from Scoop 1 concluded Phase 1 of the Bagnold Dune Campaign.

4. Key Results in this Special Issue

This special issue comprises 11 papers that together with two other recent publications associated with the Bagnold Dunes campaign in other journals [*Lapotre et al.*, 2016; *Newman et al.*, 2017] represent a significant advancement in our understanding of dunes on Mars (Table 3). We briefly review the major published results and their implications, organized by the motivating goals. Additionally, *Chojnacki and Fenton* [2017] provide a commentary on the full Bagnold Special Issue paper suite.

4.1. Activity and Morphology: Determine Current Dune Processes, Rates, and Structures

Active dunes are dynamic and ever changing sedimentary systems, the understanding of which is still an evolving research field on Earth. A key outstanding question for Mars has been reconciling the evidence

Table 3. Manuscripts Resulting From Phase 1 of the Bagnold Dune Campaign

Authors	Title (Journal)	Topic
Achilles et al. [2017]	Mineralogy of an active eolian sediment from the Namib Dune, Gale Crater, Mars *(JGR-Planets)*	The mineralogy and crystal chemistry of the Bagnold dune sands measured by CheMin, including the chemistry of the amorphous component
Bridges et al. [2017]	Martian aeolian activity at the Bagnold Dunes, Gale Crater: The view from the surface and orbit *(JGR-Planets)*	Description of morphologic changes occurring in dune surfaces and ripples observed by Curiosity, coupled with predictions from wind models and REMS data
Bridges and Ehlmann [2017] (this paper)	The Mars Science Laboratory (MSL) Bagnold Dunes Campaign, Phase I: Overview and introduction to the special issue *(JGR-Planets)*	Overview of the major guiding motivations and principal findings of the Bagnold dune campaign, Phase I, including a summary of activities, a summary of journal contributions, and a memorial tribute to Nathan Bridges
Cousin et al. [2017]	Geochemistry of the Bagnold Dune Field as observed by ChemCam and comparison with other aeolian deposits at Gale crater *(JGR-Planets)*	The chemistry of Bagnold dune sands relative to other soils in Gale crater and as a function of grain size observed by ChemCam, as well as size distribution of grains
Edwards et al. [2017]	The thermophysical properties of the Bagnold Dunes, Mars: Ground truthing orbital data *(JGR-Planets)*	Derivation of the thermophysical properties of the dune sands from REMS data, consideration of the effects of ripples and bedrock patches, and comparison to orbital data
Ehlmann et al. [2017]	Chemistry, mineralogy, and grain properties at Namib and High dunes, Bagnold dune field, Gale crater, Mars: A synthesis of Curiosity rover observations *(JGR-Planets)*	A synthesis of grain size and composition from all instruments, comparison of sands to other soils, determination of the distinct chemistries of volatile-bearing phases present in sands versus dust, and potential source rocks for the Bagnold dunes
Ewing et al. [2017]	Sedimentary processes of the Bagnold Dunes: Implications for the eolian rock record of Mars *(JGR-Planets)*	Morphometric analysis using stereo-image derived digital elevation models of the morphometry of dunes and large ripples and comparison of observed morphologies with dominant wind directions
Johnson et al. [2017]	Visible/near-infrared spectral diversity from in situ observations of the Bagnold Dune Field sands in Gale Crater, Mars *(JGR-Planets)*	The visible/near-infrared spectroscopic properties of sands with Mastcam and ChemCam passive data, including variation with grain size
Lapotre et al. [2016]	Large wind ripples on Mars: A record of atmospheric evolution (*Science*)	The description and explanation of the origin of large ripples, intermediate in size between classical ripples and large dunes
Lapotre et al. [2017b]	A probabilistic approach to remote compositional analysis of planetary surfaces *(JGR-Planets)*	The methodology underlying quantitative radiative transfer modeling to determine composition, including error bars, as applied to lab data, the composition of the Bagnold dunes, and other planetary surfaces
Lapotre et al. [2017a]	Compositional variations in sands of the Bagnold Dunes, Gale Crater, Mars, from visible-shortwave infrared spectroscopy and comparison with ground-truth from the Curiosity rover *(JGR-Planets)*	The composition and the compositional variability within the Bagnold dune field as derived from CRISM orbital remote sensing data and compared with CheMin data from *Achilles et al.* [2017]
Newman et al. [2017]	Winds measured by the Rover Environmental Monitoring Station (REMS) during the Mars Science Laboratory (MSL) rover's Bagnold Dunes Campaign and comparison with numerical modeling using MarsWRF (*Icarus*)	Compilation of REMS wind measurements made during the campaign, the study of the influence of dune topography on wind field, and comparison of observed winds to global climate models
O'Connell-Cooper et al. [2017]	APXS-derived chemistry of the Bagnold dune sands: Comparisons with Gale crater soils and the global Martian average *(JGR-Planets)*	The chemistry of Bagnold dune sands relative to other soils and as a function of grain size with APXS
Sullivan and Kok [2017]	Aeolian saltation on Mars at low wind speeds *(JGR-Planets)*	Results from computational models and lab experiments explaining how grain splash can initiate and sustain saltation on Mars even when theoretical threshold wind speeds are not sustained

that dune and ripple movement are common versus experimental and theoretical predictions that sand entrainment by the wind should be rare based on prior understanding of wind speeds and models for grain motion. Several papers address this apparent paradox. *Newman et al.* [2017] describe the first wind measurements in an active dune field on another planet, taken during southern winter solstice. The basic wind patterns were similar to that predicted by the Mars atmospheric model, Mars Weather Research and Forecasting (MarsWRF), and consisted of ~northwesterly "upslope" winds heading up the slopes of Mount Sharp during the daytime (~09:00 to ~17:30) and ~southeasterly "downslope" winds at night (~20:00 to <08:00), rotating largely clockwise between these times. The

REMS investigation on the lee side of Namib Dune revealed "blocking" of northerly winds by the dune, leaving primarily a westerly component to the daytime winds, and also a broadening of the 1 Hz wind speed distribution likely associated with lee turbulence. *Bridges et al*. [2017] discuss aeolian activity and wind speeds observed during the campaign and place these in the context of predicted wind activity and orbital measurements of the Bagnold Dune Field over longer timescales. Based on HiRISE seasonal observations and global circulation model predictions from the MarsWRF model, Curiosity investigated the dunes in the least windy time of the year. Nevertheless, change detection images from Mastcam and RMI document grain motion, one instance of slumping, and minor grainflow on the lee face of Namib dune [*Bridges et al*., 2017]. Some of the most significant events are correlated to the highest wind speeds recorded by REMS at mean friction speeds of 0.3–0.4 m s^{-1}, though these values are below the fluid threshold velocity for detachment of surface grains via wind stresses. High wind events were associated with changes in some cases, but not others, suggesting either non-aeolian triggering mechanisms or wind gusts that were not captured by the wind sensor. Such minor changes, if integrated over long time baselines, are likely representative of other locations currently and past climates generally on Mars.

To address why sand is entrained in the thin Martian atmosphere, especially given winds that only infrequently exceed the required velocity thresholds, *Sullivan and Kok* [2017] examine the physics of sand transport and use numerical simulations to study how grains mobilized sporadically between the impact and fluid wind velocity thresholds have different fates on Earth and Mars. Turbulent eddies can detach grains that are more exposed to the wind than would be the case if they were immersed in a sand bed. On Mars, where the difference between fluid and impact wind velocity thresholds is greater than on Earth (primarily because of Mars' lower gravity), grains mobilized between these speeds will eventually gain sufficient momentum during saltation to splash additional grains more vigorously than similar-sized grains achieve within an active saltation cloud on Earth. These high kinetic energy grains act as triggers that drive further saltation, resulting in a cascade of grain motion that can explain the evidence for sand movement on Mars today and seen during the dune campaign, even given wind speeds mostly below the fluid threshold. Slow ripple migration in the presence of winds of different directions should lead to more cross-oriented patterns on simple ripples; this is observed at the Bagnold dunes. Overall, this process of initiation and splashing can produce slow changes over long time periods, helping explain the observed changes without strong winds.

The larger-scale records of modern transport processes are in the morphology of the dunes themselves and superimposed ripples. The first detailed measurements of dune structures on another planet showed some important similarities and differences compared to Earth that can be tied to environmental controls on dune formation. Impact ripples and deposits from grainflow and grainfall are very similar on the two planets. Lee slopes on grainflow and grainfall deposits, representing the dynamic and static angle of repose, are 29° and 33°, respectively, similar to terrestrial measurements [*Ewing et al*., 2017]. In contrast, the meter-scale, fine-grained sinuous ripples found commonly on Martian dunes are rare on Earth. The size (10–30 cm height; ~1 m crest-to-crest spacing) and sinuous morphologic crests are inconsistent with the same formation processes as linear, smaller decimeter-scale impact ripples and suggest instead an origin analogous to that of current ripples. This bedform scale is distinguishable on Mars because of the higher kinematic viscosity of the low pressure Martian atmosphere [*Lapotre et al*., 2016]. The location and morphology of the sedimentary structures on the dune indicate that the formative winds at the time of the Curiosity's visit were from the southeast and west, with the most recent ripple-shaping wind from the southeast [*Bridges et al*., 2017; *Ewing et al*., 2017; *Newman et al*., 2017]. Based on the analysis of the orientation of impact and large ripples, this wind regime appears to have been consistent for months but does not appear to be representative of the primary dune- and ripple-shaping wind regime [*Ewing et al*., 2017].

4.2. Constrain Dune Physical and Chemical Properties and Compositional Sorting by Wind

Loose, fine-grained materials ("soils") are ubiquitous on the surface of Mars and a key question is the local versus global properties and composition. The Bagnold dunes offer a unique soil end-member: a self-organized, well-sorted collection of sand-sized materials. Grain size analysis by multiple investigators showed that the active Namib dune had grain sizes of 50–500 μm with a mode around 125 μm and lack of the silt and dust-sized fraction so common in Martian soils [*Cousin et al*., 2017;

Edwards et al., 2017; *Ehlmann et al.*, 2017; *Ewing et al.*, 2017]. Two types of grain size distributions are found; ripples near the secondary slip face of Namib Dune (Gobabeb location) are unimodal and between 50 and 350 μm, while those near High Dune's stoss base have a distinctive tail of hard-to-mobilize coarse grains [*Ewing et al.*, 2017]. There were at least five colors of grains [*Cousin et al.*, 2017; *Ehlmann et al.*, 2017]. The thermophysical properties of materials derived from REMS measurements on the ground are consistent with this size range, with prior data from orbit, and are not affected by the ripple structures [*Edwards et al.*, 2017]. *Edwards et al.* [2017] note that previous orbital IR measurements of other dunes that indicated a coarser grain size may be explained by intrapixel mixing between sand-sized materials in the dunes and high thermal inertia bedrock.

New probabilistic methods were derived for improved quantification of mineralogy from orbit from visible/shortwave-infrared data [*Lapotre et al.*, 2017b]. Use of these methods with orbital CRISM spectra to estimate the composition of Namib dune [*Lapotre et al.*, 2017a] and previous orbital modeling efforts using data from the Thermal Emission Spectrometer (TES) closely matched CheMin-derived mineralogies [*Achilles et al.*, 2017; *Lapotre et al.*, 2017a]. The crystalline mineralogy of the dunes consists of feldspar, two pyroxenes, olivine and small amounts of anhydrite, quartz, magnetite, ilmenite, and hematite, similar to the mineralogy of the Rocknest fines [*Achilles et al.*, 2017]. However, the chemistry is considerably different. The dunes are more Si, Mg, Fe, and Ni enriched relative to other Gale crater soils [*Cousin et al.*, 2017; *Ehlmann et al.*, 2017; *O'Connell-Cooper et al.*, 2017]. As with the Rocknest soils [*Leshin et al.*, 2013], the dune sands have among the highest content of C- and N-species relative to other Gale crater materials [*Ehlmann et al.*, 2017; *Sutter et al.*, 2017]. However, all rover instruments show that the dunes are substantially depleted in H, S, and Cl. Weight percent H_2O in the Bagnold dune sands is ~1%, with the majority released after 400°C, while weight percent water in the previously measured Martian soils was 2–3 wt %, with nearly all water released by 400°C [*Ehlmann et al.*, 2017; *Sutter et al.*, 2017]. Given the lack of volatile-bearing phases in the crystalline fraction, it is the composition of the ~40 wt % X-ray amorphous phase that drives the chemical differences [*Achilles et al.*, 2017; *Ehlmann et al.*, 2017]. This may be due to two fundamentally different volatile reservoirs in the Mars soil, segregated by grain size: an Fe, S, and Cl-enriched and low-temperature-release-H_2O-enriched amorphous material in dust/silt, largely absent in the Bagnold dunes, and the volatiles in the Bagnold sands, which are S and Cl poor and with H_2O/OH more tightly bound as hydroxylated phases or as waters within glasses [*Ehlmann et al.*, 2017].

Grain size influences composition with the coarsest fractions being most mafic. This is observed in APXS and ChemCam chemical data of the discarded piles of sieved sands [*Cousin et al.*, 2017; *O'Connell-Cooper et al.*, 2017; *Ehlmann et al.*, 2017] as well as in mast-based rover remote sensing [*Johnson et al.*, 2017]. *Johnson et al.* [2017] use Mastcam multispectral imaging (445–1013 nm) and ChemCam passive point spectroscopy (400–840 nm) and find that the finest sands have spectra consistent with a combination of crystalline ferrous and ferric materials. In contrast the coarser sands are darker and bluer, consistent with a greater proportion of mafic minerals such as pyroxene and olivine. The spectra are relatively dust-free, consistent with orbital data [*Seelos et al.*, 2014; *Lapotre et al.*, 2017a] and with ongoing aeolian activity that would remove dust in suspension.

4.3. Collect Knowledge That Informs the Provenance of Sediments and Interpretation of Past Dune Processes Preserved in the Martian Sedimentary Rock Record

Fundamental for understanding sedimentary systems is knowing the source, or in many cases, multiple sources, that contribute to the population of sand and other grains found in extant deposits and in the rock record. This is particularly true for Mars, where there is a poor understanding of aeolian sand migration pathways and the longevity of grains transported by saltation. Understanding the modern processes driving the observed physical and compositional characteristics of the modern aeolian record is key to understanding the ancient sedimentary rock record, i.e., disentangling the environmental history of transport, sorting, and weathering or diagenetic alteration. The modern morphology of centimeter-height impact ripples, decimeter-height large ripples, and meters to tens of meter-scale dunes would be translated to cross stratification at multiple scales in the rock record. In the upper ~10 cm exposure in the Gobabeb scuff, fairly conventional impact ripple stratification was seen with millimeter-scale laminae and inverse grading. Over larger scales, the other observed morphologies might be preserved. Decimeter-thick, m-scale spaced cross sets

grouped into larger cross sets by the migration of the dune may even serve as an indicator of paleopressure, since a fluid drag model for their formation predicts smaller ripple wavelengths for higher atmospheric pressure [*Lapotre et al*., 2016; *Ewing et al*., 2017].

Chemical and mineralogic data of dune sands are crucial to understanding sand provenance as well as the postdepositional diagenetic changes that transform Martian aeolian bedforms to Martian rocks. Relative to bedrock at Gale crater, the Bagnold dunes are broadly similar, i.e., basaltic [*O'Connell-Cooper et al*., 2017]. But the sedimentary rocks are enriched in S and Cl, pointing either to a contribution of fine dust as the bedforms become immobile and/or the infiltration of waters and precipitation of cements as the dune sands are lithified [*Ehlmann et al*., 2017; *O'Connell-Cooper et al*., 2017]. Another key question is the source of the dunes: are they newly eroded materials from igneous bedrock or eroded and reworked earlier generations of sandstones? The major elemental chemistry of the Bradbury sandstones measured by Curiosity is sufficiently different that they are unlikely to be a major source of the Bagnold dunes. Reworking of the nearby Stimson sandstone is possible as the elemental chemistries are similar, but the Stimson has little to no olivine in contrast to the dunes. Thus, this suggests that the origin of the dunes is erosion of the olivine-bearing walls of Gale crater [*Buz et al*., 2017] and/or erosion of sandstones yet-to-be-encountered on the rover's ascent of Mount Sharp [*Ehlmann et al*., 2017].

5. Summary and Outstanding Questions

Major findings of the Bagnold dune campaign include the following:

1. The first measurements of winds and activity within a dune field on another planet.
2. The discovery of bedforms that appear to be specifically characteristic of Mars' low-pressure atmosphere, which may be analogous to current ripples.
3. The elucidation of a new mechanism that successfully explains saltation and bedform migration on Mars even when wind velocities are below the fluid threshold.
4. The Gobabeb sands have the lowest S and Cl content of any fines measured on Mars.
5. The crystalline mineralogy of Martian sands and soils is similar and basaltic, but the substantial (30–40%) amorphous fraction has at least two components that comprise distinct reservoirs for volatiles.
6. Compositional sorting by winds according to grain size subtly influences the major element chemistry of active sands.
7. Due to their high olivine content, the source of the dunes is likely the walls of Gale crater or eroded sandstones further up Mount Sharp rather than rocks visited by the rovers so far.

Key outstanding questions, amplified by the results of the campaign, include the following:

1. What are dune and ripple migration rates and fluxes in higher wind seasons?
2. What are the major structures on Martian longitudinal dunes and how do these compare to the barchanoidal dunes near Gobabeb, dunes elsewhere on Mars, and longitudinal dunes on Earth?
3. Why do the longitudinal dunes near the center of the dune field have a distinctive spectral signature in shortwave infrared remote sensing data relative to barchan dunes at the margins of the field?
4. From what sources do the multicolored grains making up the Bagnold dunes derive, and how much contribution is from local bedrock?
5. Is the D/H isotopic ratio of high temperature, more tightly bound H_2O in sands the same as lower temperature waters released from Rocknest fines, or do the isotopes indicate distinctive ancient and modern reservoirs?
6. Is the $\delta^{13}C$ isotopic signature distinctive in Bagnold sands versus Rocknest fines, and what does this indicate about the nature and origin of the C-bearing component in Martian fines?
7. What is the isotopic composition of the N reservoir in the sand?

As of the writing of this overview, the rover had just completed the Bagnold Dunes Campaign, Phase 2, investigation at the longitudinal dunes, which will add to the body of knowledge to address these and other questions. Collectively, the results from Curiosity's Bagnold Dune Campaign have provided a rich data set and fundamental insights into how winds shape the evolution of surfaces and the sedimentary rock record across planets.

Appendix A: A Dedication: Nathan Bridges, 1966–2017

We, Nathan Bridges and Bethany Ehlmann, were the coordinators of the MSL Aeolian Working Group, which planned the activities of the Bagnold campaign. During the writing of the special issue, Nathan passed away unexpectedly on 26 April 2017. He is survived by wife Karen, daughter Sarah, and son Matthew.

Nathan was an internationally recognized leader in geomorphology, specializing in planetary aeolian processes (Figure A1). His recent work focused on ventifacts, sand dunes, the activity of sands on Mars, and the movement of tholin-rich grains on Titan. Nathan was a member of several mission teams, including Mars Pathfinder, the Mars Reconnaissance Orbiter HiRISE investigation, the Mars Science Laboratory ChemCam investigation, and the upcoming Mars-2020 rover. Nathan earned a BA in Geology from the University of Colorado (1989), an MS in Geology from Arizona State University (1992), and a PhD in Geology from the University of Massachusetts (1997). He spent 12 years at NASA's Jet Propulsion Laboratory in Pasadena, California, before joining The Johns Hopkins University Applied Physics Laboratory in 2009.

In addition to his scientific acumen, Nathan was an extraordinarily generous person, devoted to advancing aeolian research via numerous collaborations, eager to share knowledge and learn as part of other collaborations, and committed to advocating for science with the American Geophysical Union. An unselfish and careful collaborator on scientific work, he was a kind and thoughtful presence in the sometimes rough and tumble world of mission science. He was also talented in connecting planetary science and MSL to those outside the field. Figure A2 shows Nathan in his element in the heart of the dunes of Namibia on a recent field trip, sharing his knowledge and joy in the study of aeolian processes with others.

Thus, this Bagnold Dunes Campaign, Phase I, *JGR-Planets* special issue is dedicated to Nathan Bridges: we will greatly miss him as we continue the explorations he helped pioneer. We have named a key longitudinal dune examined in the Phase II campaign Nathan Bridges Dune, melding Ralph Bagnold's legacy and Nathan Bridges's legacy within the first active dune field explored on another planet. We think that Nathan would be pleased with this intertwining.

Figure A1. Nathan Bridges at a ChemCam team meeting dinner in Paris in June 2012 (photo by Horton Newsom).

Figure A2. Nathan Bridges at the International Geological Congress Namib Desert field trip in August 2016, pondering the origin of the left-to-right-trending lineations (photo by Dave Rubin).

Acknowledgments
Many thanks to MSL's Aeolian Working Group for their conception of the campaign as well as MSL's entire operations team for its implementation. Particular thanks to Lori Fenton and Matt Chojnacki for serving as editors for the Bagnold special issue and to the *JGR-Planets* editors and staff, particularly Steve Hauck and Carol Manix, for their support. The formal reviews by Kirby Runyon and Nick Lancaster and readings of drafts by Agnes Cousin, Mathieu Lapotre, Jason Van Beek, and Ashwin Vasavada improved this manuscript and are appreciated. Thanks to Horton Newsom and Dave Rubin for the photos of Nathan Bridges and Stephen Bagnold for the photo of Ralph Bagnold. Bridges was funded by NASA as a Co-I on the MSL ChemCam team. Ehlmann was funded by NASA's MSL Participating Scientist program. This review contains no new data, and the reader should refer to the data statements in the manuscripts cited. All data from the MSL mission are available online at the NASA Planetary Data System Geosciences Node.

References

Achilles, C. N., et al. (2017), Mineralogy of an active eolian sediment from the Namib Dune, Gale Crater, Mars, *J. Geophys. Res. Planets*, *122*, doi:10.1002/2017JE005262.

Anderson, R. B., and J. F. Bell III (2010), Geologic mapping and characterization of Gale Crater and implications for its potential as a Mars Science Laboratory landing site, *Marsyas*, *5*, 76–128, doi:10.1555/mars.2010.0004.

Anderson, R. C., et al. (2012), Collecting samples in Gale Crater, Mars: An overview of the Mars Science Laboratory sample acquisition, sample processing and handling system, *Space Sci. Rev.*, doi:10.1007/s11214-012-9898-9.

Arvidson, R. E., et al. (2017), Mars Science Laboratory Curiosity rover megaripple crossings up to sol 710 in Gale Crater, *J. Field Robotics*, *34*, 495–518, doi:10.1002/rob.21647.

Ayoub, F., J.-P. Avouac, C. E. Newman, M. I. Richardson, A. Lucas, S. Leprince, and N. T. Bridges (2014), Threshold for sand mobility on Mars calibrated from seasonal variations in sand flux, *Nature Comm.*, *5*, 5096, doi:10.1038/ncomms6096.

Bagnold, R. A. (1941) *The Physics of Blown Sand and Desert Dunes*, Methuen & Co., Ltd., London.

Bagnold, R. A. (1990) *Sand, Wind, and War: Memoirs of a Desert Explorer*, p. 209, The Univ. of Arizona Press, Tucson.

Bell, J. F., III, et al. (2017), The Mars Science Laboratory Curiosity Rover Mast Camera (Mastcam) Instruments: Pre-flight and in-flight calibration, validation, and data archiving, *Earth Space Sci.*, *4*, doi:10.1002/2016EA000219.

Bish, D. L., et al. (2013), X-ray diffraction results from Mars Science Laboratory: Mineralogy of Rocknest at Gale Crater, *Science*, *341*(6153), 1238932, doi:10.1126/science.1238932.
Blake, D., et al. (2012), Characterization and calibration of the CheMin mineralogical instrument on Mars Science Laboratory, *Space Sci. Rev.*, doi:10.1007/s11214-012-9905-1.
Blake, D. F., et al. (2013), Curiosity at Gale Crater, Mars: Characterization and analysis of the Rocknest sand shadow, *Science*, *341*, doi:10.1126/science.1239505.
Bourke, M. C., K. S. Edgett, and B. A. Cantor (2008), Recent aeolian dune changes on Mars, *Geomorphology*, *94*, 247–255, doi:10.1016/j.geomorph.2007.05.012.
Bridges, N. T., R. Greeley, A. F. C. Haldemann, K. E. Herkenhoff, M. Kraft, T. J. Parker, and A. W. Ward (1999), Ventifacts at the Pathfinder landing site, *J. Geophys. Res.*, *104*, 8595–8615, doi:10.1029/98JE02550.
Bridges, N. T., et al. (2012), Planet-wide sand motion on Mars, *Geology*, *40*(1), 31–34, doi:10.1130/G32373.1.
Bridges, N. T., et al. (2017), Martian aeolian activity at the Bagnold Dunes, Gale Crater: The view from the surface and orbit, *J. Geophys. Res. Planets*, *122*, doi:10.1002/2017JE005263.
Buz, J., B. L. Ehlmann, L. Pan, and J. P. Grotzinger (2017), Mineralogy and stratigraphy of the Gale Crater rim, wall, and floor units, *J. Geophys. Res. Planets*, *122*, doi:10.1002/2016JE005163.
Chojnacki, M., and L. K. Fenton (2017), The geologic exploration of the Bagnold dune field at Gale crater by the Curiosity rover, *J. Geophys. Res. Planets*, *122*, 2216–2222, doi:10.1002/2017JE005455.
Cousin, A., et al. (2015), Compositions of sub-millimeter-size clasts and fine particles in the Martian soils at Gale: A window into the production of soils, *Icarus*, *249*, 22–42, doi:10.1016/j.icarus.2014.04/052.
Cousin, A., et al. (2017), Geochemistry of the Bagnold Dune Field as observed by ChemCam and comparison with other aeolian deposits at Gale crater, *J. Geophys. Res. Planets*, doi:10.1002/2017JE005261.
Edgar, L. A., et al. (2012), Stratigraphic architecture of bedrock reference section, Victoria crater, Meridiani Planum, Mars, in *Sedimentary Geology of Mars*, *SEPM Special Publication*, vol. 102, edited by J. Grotzinger and R. Milliken, pp. 195–209.
Edgett, K. S., et al. (2012), Curiosity's Mars Hand Lens Imager (MAHLI) investigation, *Space Sci. Rev.*, doi:10.1007/s11214-012-9910-4.
Edwards, C. et al., (2017), The thermophysical properties of the Bagnold Dunes, Mars: Ground-truthing orbital data, http://arxiv.org/abs/1711.10699.
Ehlmann, B. L., et al. (2017), Chemistry, mineralogy, and grain properties at Namib and High Dunes, Bagnold Dune Field, Gale Crater, Mars: A synthesis of Curiosity rover observations, *J. Geophys. Res. Planets*, *122*, doi:10.1002/2017JE005267.
Ewing, R. C., et al. (2017), Sedimentary processes of the Bagnold Dunes: Implications for the eolian rock record of Mars, *J. Geophys. Res. Planets*, *122*, doi:10.1002/2017JE005324.
Gellert, R., and B. C. Clark (2015), In-situ compositional measurements of rocks and soils with the Alpha Particle X-ray Spectrometer on NASA's Mars rovers, *Elements*, *11*, 39–44, doi:10.2113/gselements.11.1.39.
Golombek, M., K. Robinson, A. McEwen, N. Bridges, B. Ivanov, L. Tornabene, and R. Sullivan (2010), Constraints on ripple migration at Meridiani Planum from Opportunity and HiRISE observations of fresh craters, *J. Geophys. Res.*, *115*, E00F08, doi:10.1029/2010JE003628.
Gomez-Elvira, J., et al. (2012), REMS: The environmental sensor suite for the Mars Science Laboratory Rover, *Space Sci. Rev.*, *170*, 583–640, doi:10.1007/s11214-012-9921-1.
Greeley, R., N. T. Bridges, R. O. Kuzmin, and J. E. Laity (2002), Terrestrial analogs to wind related features at the Viking and Pathfinder landing sites on Mars, *J. Geophys. Res.*, *107*(E1), 5-1–5-22, doi:10.1029/2000JEE001481.
Greeley, R., et al. (2006), Gusev crater: Wind related features and processes observed by the Mars Exploration Rover Spirit, *J. Geophys. Res.*, *111*. E02S09, doi:10.1029/2005JE002491.
Greeley, R., et al. (2008), Columbia Hills, Mars: Aeolian features seen from the ground and orbit, *J. Geophys. Res.*, *113*, E06S06, doi:10.1029/2007JE002971.
Grotzinger, J. P., J. Crisp, A. R. Vasavada, R. C. Anderson, C. J. Baker, R. Barry, D. F. Blake, P. Conrad, K. S. Edgett, and B. Ferdowski (2012), Mars Science Laboratory mission and science investigation, *Space Sci. Rev.*, *170*, 5–56, doi:10.1007/s11214-012-9892-2.
Grotzinger, J., S. Gupta, M. Malin, D. Rubin, J. Schieber, K. Siebach, D. Sumner, K. Stack, A. Vasavada, and R. Arvidson (2015), Deposition, exhumation, and paleoclimate of an ancient lake deposit, Gale Crater, Mars, *Science*, *350*(6257), aac7575, doi:10.1126/science.aac7575.
Grotzinger, J. P., et al. (2005), Stratigraphy and sedimentology of a dry to wet eolian depositional system, Burns formation, Meridiani Planum, Mars, *Earth Planet. Sci. Lett.*, *240*, 11–72.
Jerolmack, D. J., D. Mohrig, J. P. Grotzinger, D. A. Fike, and W. A. Watters (2006), Spatial grain size sorting in eolian ripples and estimation of wind conditions on planetary surfaces: Application to Meridiani Planum, Mars, *J. Geophys. Res.*, *111*, E12S02, doi:10.1029/2005JE002544.
Johnson, J. R., et al. (2017), Visible/near-infrared spectral diversity from in situ observations of the Bagnold Dune Field sands in Gale Crater, Mars, *J. Geophys. Res. Planets*, *122*, doi:10.1002/2016JE005187.
Lane, M. D., and P. R. Christensen (2013), Determining olivine composition of basaltic dunes in Gale Crater, Mars, from orbit: Awaiting ground truth from Curiosity, *Geophys. Res. Lett.*, *40*, 3517–3521, doi:10.1002/grl.50621.
Lapotre, M. G. A., B. L. Ehlmann, and S. E. Minson (2017a), A probabilistic approach to remote compositional analysis of planetary surfaces, *J. Geophys. Res. Planets*, *122*, 983–1009, doi:10.1002/2016JE005248.
Lapotre, M. G. A., B. L. Ehlmann, S. E. Minson, R. E. Arvidson, F. Ayoub, A. A. Fraeman, R. C. Ewing, and N. T. Bridges (2017b), Compositional variations in sands of the Bagnold Dunes, Gale Crater, Mars, from visible-shortwave infrared spectroscopy and comparison with ground truth from the Curiosity rover, *J. Geophys. Res. Planets*, *122*, doi:10.1002/2016JE005133.
Lapotre, M., et al. (2016), Large wind ripples on Mars: A record of atmospheric evolution, *Science*, *353*, 55–58.
Le Deit, L., E. Hauber, F. Fueten, M. Pondrelli, A. P. Rossi, and R. Jaumann (2013), Sequence of infilling events in Gale Crater, Mars: Results from morphology, stratigraphy, and mineralogy, *Journal of Geophysical Research, Planets*, *118*, 2439–2473, doi:10.1002/2012JE004322.
Leshin, L. A., et al. (2013), Volatile, isotope, and organic analysis of Martian fines with the Mars Curiosity rover, *Science*, *341*(6153), 1238937.
Mahaffy, P. R., et al. (2012), The sample analysis at Mars investigation and instrument suite, *Space Science Reviews*, doi:10.1007/s11214-012-9879-z.
Maki, J., et al. (2012), The Mars Science Laboratory engineering cameras, *Space Science Reviews*, *170*, doi:10.1007/s11214-012-9882-4.
Malin, M. C., et al. (2017), The Mars Science Laboratory (MSL) mast cameras and descent imager: I. Investigation and instrument descriptions, *Earth Space Sci.*, doi:10.1002/2016EA000252.
Malin, M. C., and K. S. Edgett (2000), Sedimentary rocks of early Mars, *Science*, *290*, 1927–1937, doi:10.1126/science.290.5498.1927.
Marsusky, H. (1973), An overview of geological results from Mariner 9, *Journal of Geophysical Research*, *78*(20), 4009–4030, doi:10.1029/JB078i020p04009.

Maurice, S., et al. (2012), The ChemCam instrument suite on the Mars Science Laboratory (MSL) rover: Science objectives and mast unit description, *Space Science Reviews*, *170*, 95–166, doi:10.1007/s11214-012-9912-2.
Milliken, R. E., J. P. Grotzinger, and B. J. Thomson (2010), Paleoclimate of Mars as captured by the stratigraphic record in Gale Crater, *Geophysical Research Letters*, *37*, L04201, doi:10.1029/2009GL041870.
Milliken, R. E., R. C. Ewing, W. W. Fischer, and J. Hurowitz (2014), Wind-blown sandstones cemented by sulfate and clay minerals in Gale Crater, Mars, *Geophys. Res. Lett.*, *41*, 1149–1154, doi:10.1002/2013GL059097.
Minitti, M. E., et al. (2013), MAHLI at the Rocknest sand shadow: Science and science-enabling activities, *Journal of Geophysical Research, Planets*, *118*, 2338–2360, doi:10.1002/2013JE004426.
Mitrofanov, I. G., et al. (2012), Dynamic Albedo of Neutrons (DAN) Experiment Onboard NASA's Mars Science Laboratory, *Space Sci. Rev.*, *170*, 559–582, doi:10.1007/s11214-012-9924.
Newman, C., et al. (2017), Winds measured by the Rover Environmental Monitoring Station (REMS) during the Mars Science Laboratory (MSL) rover's Bagnold Dunes Campaign and comparison with numerical modeling using MarsWRF, *Icarus*, *291*, 203–231.
O'Connell-Cooper, C. D., J. G. Spray, L. M. Thompson, R. Gellert, J. A. Berger, N. I. Boyd, E. D. Desouza, G. M. Perrett, M. Schmidt, and S. J. VanBommel (2017), APXS-derived chemistry of the Bagnold dune sands: Comparisons with Gale crater soils and the global martian average, *Journal of Geophysical Research, Planets*, *122*, doi:10.1002/2017JE005268.
Pelkey, S. M., B. M. Jakosky, and P. R. Christensen (2004), Surficial properties in Gale Crater, Mars, from Mars Odyssey THEMIS data, *Icarus*, *167*, 244–270, doi:10.1016/j.icarus.2003.09.013.
Rogers, A. D., and J. L. Bandfield (2009), Mineralogical characterization of Mars Science Laboratory candidate landing sites from THEMIS and TES data, *Icarus*, *203*, 437–453.
Sanin, A. B., et al. (2015), Data processing of the active neutron experiment DAN for a Martian regolith investigation, *Nuclear Inst. Methods Phys. Res. Sec. A*, *789*, 114–127.
Scott, D.H. and M.H. Carr (1978) Geologic map of Mars. United States Geological Survey Atlas of Mars #I-1082.
Seelos, K. D., F. P. Seelos, C. E. Viviano-Beck, S. L. Murchie, R. E. Arvidson, B. L. Ehlmann, and A. A. Fraeman (2014), Mineralogy of the MSL Curiosity landing site in Gale crater as observed by MRO/CRISM, *Geophys. Res. Lett.*, *41*, 4880–4887, doi:10.1002/2014GL060310.
Silvestro, S., L. K. Fenton, D. A. Vaz, N. T. Bridges, and G. G. Ori (2010), Ripple migration and dune activity on Mars: Evidence for dynamic processes, *Geophysical Research Letters*, *37*, L20203, doi:10.1029/2010GL044743.
Silvestro, S., D. A. Vaz, R. C. Ewing, A. P. Rossi, L. K. Fenton, T. I. Michaels, J. Flahaut, and P. E. Geissler (2013), Pervasive aeolian activity along rover Curiosity's traverse in Gale Crater, Mars, *Geology*, *41*(4), 483–486, doi:10.1130/G34162.1.
Sullivan, R., R. Arvidson, J. Bell, R. Gellert, M. Golombek, R. Greeley, K. Herkenhoff, J. Johnson, S. Thompson, and P. Whelley (2008), Wind-driven particle mobility on Mars: Insights from Mars Exploration Rover observations at El Dorado and surroundings at Gusev Crater, *Journal of Geophysical Research*, *113*, E06S07, doi:10.1029/2008JE003101.
Sullivan, R., and J. F. Kok (2017), Aeolian saltation on Mars at low wind speeds, *Journal of Geophysical Research, Planets*, *122*, doi:10.1002/2017JE005275.
Sullivan, R., et al. (2005), Aeolian processes at the Mars Exploration rover Meridiani Planum landing site, *Nature*, *436*, 58–61.
Sutter, B., et al. (2017), Evolved gas analyses of sedimentary rocks and eolian sediment in Gale Crater, Mars: Results of the Curiosity rover's Sample Analysis at Mars (SAM) Instrument from Yellowknife Bay to the Namib Dune, *J. Geophys. Res. Planets*, *122*, doi:10.1002/2016JE005225.
Tanaka, K. L., J. A. Skinner, Jr., J. M. Dohm, R. P. Irwin, III, E. J. Kolb, C. M. Fortezzo, T. Platz, G. G. Michael, and T. M. Hare (2014), Geologic map of Mars, Scale 1:20,000,000, U.S. Geological Survey Scientific Investigations Map SIM 3292.
Wiens, R. C., et al. (2012), The ChemCam instrument suite on the Mars Science Laboratory (MSL), body unit and combined system tests, *Space Sci. Rev, Rover*, doi:10.1007/s11214-012-9902-4.
Zurek, R. W., and L. J. Martin (1993), Interannual variability of planet-encircling dust storms on Mars, *J. Geophys. Res.*, *98*(E2), 3247–3259, doi:10.1029/92JE02936.